Journal of Natural Disaster Science, Volume 38, Number 2, 2017, pp145-164

Development and Application of a Building Group Destruction Probability Model Based on the Great East Japan Earthquake Tsunami Experience

Ryoichi Yanagawa*

*Department of Civil Engineering, National Institute of Technology, Kagawa College

(Received: Dec.20, 2016 Accepted: Sep.13, 2017)

Abstract

This study examined the regional spatial characteristics of tsunami flooding and building damage using geographic information systems. An analytical model that evaluates total building destruction risk was developed using building damage data from coastal areas in Iwate Prefecture. Building density characteristics in the study area were categorized into four types of environments: (1) many isolated buildings, (2) combination of isolated and neighboring buildings, (3) combination of neighboring and surrounding buildings, and (4) many neighboring buildings. Many isolated buildings were located along the narrow, low-lying areas facing the Pacific Ocean. In comparison, higher building densities were observed along the inner part of the enclosed gulf topography. Most buildings located near the shoreline collapsed. Farther inland, a higher percentage of buildings experienced *half-collapse* or *no-damage*. Closer inspection of the varying spatial distribution characteristics and resultant building damage among the 27 target areas led to the identification of several key indicators for predicted building damage including the structure, use, and density of the affected building and the extent of tsunami inundation. Based on the building damage characteristics following the 2011 tsunami, a building group destruction probability model was developed and verified. The proposed model successfully estimated building collapse ratios using the available data.

Keywords: Great East Japan Earthquake, Tsunami, Building damage, Damage estimation, Iwate Prefecture

1. Introduction

The Great East Japan Earthquake (GEJE) occurred on March 11, 2011. The Japan Weather Association located the epicenter of the earthquake at 38.103°N latitude and 142.860°E longitude. Its moment magnitude reached 9.0 and its maximum seismic intensity reached 7 in Kurihara City in Miyagi Prefecture (Japan Meteorological Agency, 2012). The tsunami caused by the GEJE also had significant impacts. In Iwate Prefecture, a maximum run-up height of 39.71 m was directly observed during the 2011 tsunami (Mori et al., 2012), whereas results from geographic information system (GIS) analyses estimated a maximum run-up height of 49.8 ± 0.2 m (Yanagawa et al., 2016). On March 11, 2014, Japan's National Police Agency confirmed 18,517 dead and missing persons within 12 prefectural and city government jurisdictions as a result of the tsunami caused by the GEJE and its aftershocks. Iwate Prefecture was especially impacted with more than 6,000 dead and missing persons and 23,000 collapsed homes. More than 45,000 buildings in Iwate Prefecture were inundated by the tsunami (Yanagawa et al., 2014a), and various reports noted that most buildings

were flooded or extremely damaged (Arikawa, 2012; Hiraishi, 2012; Inukai et al., 2012; Kawasaki, 2012; Suppasri et al., 2012; Suzuki et al., 2012). In addition, various purpose-developed analytical techniques were applied to quantitatively clarify the extent of building damage, which could only previously be ascertained qualitatively (Charvet et al., 2014; Gokon et al., 2016; Koshimura et al., 2012a; Koshimura et al., 2012b; Macabuag et al., 2016; Narita et al., 2015). Used as an indicator of house damage, Figure 1 shows Hatori's destruction ratio (Hatori, 1964) measured at 24 different coastal locations. Kuji Bay in the north and Miyako Bay in the middle had relatively low Hatori destruction ratios of 56.3% and 71.2%, respectively. Each of the other areas had significantly higher Hatori destruction ratios. Among them, 15 areas had ratios over 90%, indicating that most or all of the buildings were washed away or completely destroyed (Yanagawa et al., 2014b).

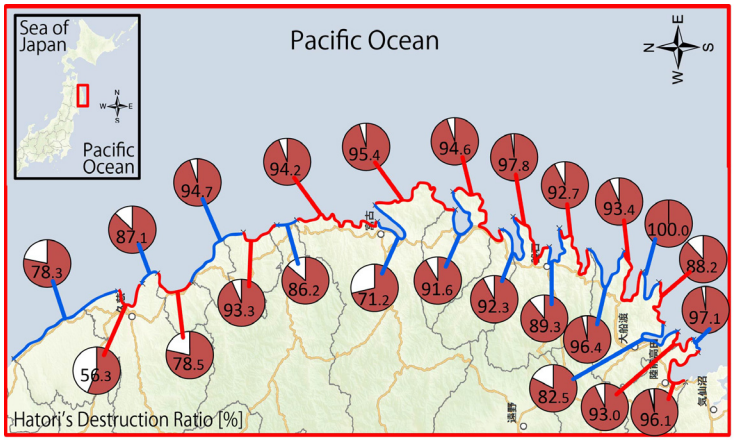

Fig. 1. Building damage in 24 regional coastal areas characterized by Hatori's destruction ratio

The extent of building damage is likely to be affected by a number of different factors related to coastal morphology (e.g., elevation, bay size, existence of coastal protection facilities); building features (e.g., shoreline setback, number of stories, structure type, building density); and tsunami wave characteristics (e.g., height, velocity, power, dominant direction, overtopping height of facilities). TABLE 1 provides a partial list of potential explanatory factors affecting building damage. Of these factors, the building structure type, the building density, and the extent of tsunami inundation are most readily available for measurement. The development of an evaluation method based on such readily accessible information is considered useful when conducting tsunami risk assessment. Related research was carried out by Narita et al. (2015), who presented a tsunami fragility curve corresponding to the topographical features by utilizing principal component analysis and cluster analysis. However, their study only focused on severe tsunami damage (washed away), and their consideration of cases with less damage was insufficient. Charvet et al. (2014) and Macabuag et al. (2016) created a fragility curve using various target areas, explanatory variables, and analytical methods, but they did not conduct damage analysis in the coastal area of Iwate Prefecture.

TABLE 1. Potential factors affecting tsunami-related building damage

Items		Common collection method	Place to obtainin Japan	Difficulty of obtaining
Geography	Elevation on land	Data download	Public agency	Easy
	Depth at sea	Data download	Public agency	Easy
	Size of the bay	Spatial analysis	Individual	Difficult
	Shoreline length	Spatial analysis	Individual	Difficult
	State of the land	Site reconnaissance	Individual	Difficult
	Coastal protection facility	Document Site reconnaissance	Public agency, Local municipality	Easy
	Distance to the shoreline	Spatial analysis	Individual	Easy
Building	Number of stories	Data download Site reconnaissance	Public agency, Local municipality Individual	Easy
	Structure type	Data download Site reconnaissance	Public agency, Local municipality Individual	Easy
	Density	Site reconnaissance	Individual	Easy
Tsunami	Wave height	Numerical model	Public agency, Local municipality	Easy
	Inundation area	Numerical model Site reconnaissance	Public agency, Local municipality	Easy
	Wave velocity	Numerical model	Public agency	Difficult
	Wave power	Numerical model	Public agency	Difficult
	Wave direction	Numerical model	Public agency	Difficult
	Overtopping height at the facility	Numerical model	Public agency	Difficult

In this study, regional spatial characteristics regarding the extent of tsunami inundation and building damage caused by the tsunami were examined using GIS. Additionally, an analytical model that evaluates total building destruction risk was developed using building damage data from Iwate Prefecture.

2. Data Collection and Methods

For each of the 27 regional areas on the Iwate coast, data regarding the building structure type, building density, extent of tsunami inundation (i.e., spatial distribution and height), and resultant building damage were overlaid in a GIS within a computational mesh. The Geospatial Information Authority of Japan (2012) provided elevation data after the GEJE as a lattice-shaped mesh with a spatial resolution of approximately 5 m (0.2 seconds in scale). Elevation data for each building considered in this study were applied using data from the nearest location.

Tsunami inundation and building damage characteristics in each area were examined. The maximum tsunami inundation for each building was calculated, and the relationship between destruction types and building features was considered. Based on these findings, a probability model was developed to predict the total building destruction risk for a target building using the three indicators: building structure type, building density, and extent of tsunami inundation. The accuracy of the model was then validated in the Iwate coastal area.

2.1 Building Structure Type

Building characteristics, including the structure type, were obtained from a disaster survey conducted by Japan's Ministry of Land, Infrastructure, Transport, and Tourism (MLIT) in 2011. Specifically, this disaster survey recorded the building location (in latitude and longitude), building use (*residential*, *apartment complex*, *public institution*, *plant*, *commercial building*, *barn*, etc.), and building structure (*reinforced concrete*, *steel*, *wood*, and *other/unknown*). These data were used in the analysis of this study.

2.2 Building Density

The building density was defined as the number of buildings within a 20-m radius from the center of the target building. The site area per house was approximately 250 to 300 m^2 (one side is approximately 16 to 17 m long), and the straight distance to the adjacent building was approximately within 20 m; thus, the threshold was set at 20 m. In the coastal area of Iwate Prefecture, there were eight or more buildings within a 20-m radius zone from the target in densely populated residential areas. Similarly, two to four buildings were located in areas that were relatively larger spaced. The relationship between the density expressed by this method and the denseness actually experienced was qualitatively good. A building density of zero indicates no other buildings within the target radius; a building density of 10 indicates 10 buildings within the target radius. Based on these direct building densities, three general building density categories were defined: (1) *isolated* with no buildings around the target, (2) *neighboring* with 1–3 buildings around the target, and (3) *surrounding* with ≥4 buildings around the target. Figure 2 depicts the stepwise building density estimation procedure used in this study. This process concurrently considered building structure and use.

Fig. 2. Building density estimation procedure: **1** enter building information in GIS, **2** set buffer zone radius to 20 m, **3** count building numbers within each buffer zone

2.3 Extent of Tsunami Inundation

The numerical model was used to estimate the maximum tsunami inundation area and height by focusing on the 20 coastal areas within the study area and by using information provided by the Iwate Prefecture Tsunami Disaster Prevention Technical Committee (Iwate Prefecture 2011–2012). Figure 3 shows the 20 coastal areas that were used to support the calculations. TABLE 2 contains the specifications of the tsunami inundation numerical model.

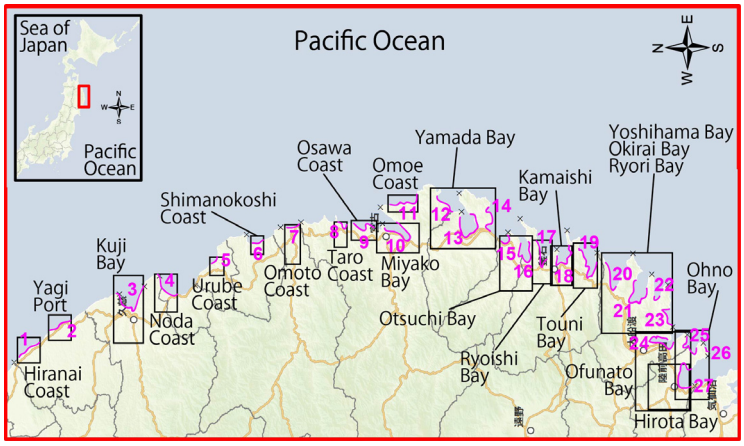

Fig. 3. Tsunami inundation area calculation domains (designated by a rectangular border); numbers in the figure indicate the 27 target areas in TABLE 3 and TABLE 4

TABLE 2. Numerical model configuration for 2011 Tohoku tsunami by Iwate Prefecture

Item	Setting	
Calculation Area	Name of Bay, Coast	Affiliated City in Iwate Prefecture
	Hiranai Coast, Yagi Port	Hirono Town
	Kuji Bay	Kuji City
	Noda Coast	Noda Village
	Urube Coast	Fudai Village
	Shimanokoshi Coast	Tanohata Village
	Omoto Coast	Iwaizumi Town
	Taro Coast, Osawa Coast, Miyako Bay, Omoe Coast	Miyako City
	Yamada Bay	Yamada Town
	Otsuchi Bay	Otsuchi Town
	Ryoishi Bay, Kamaishi Bay, Touni Bay	Kamaishi City
	Yoshihama Bay, Okirai Bay, Ryori Bay, Ofunato Bay	Ofunato City
	Ohno Bay, Hirota Bay	Rikuzentakata City
Basic Equation and Solving Method	Based on the Non-Linear Long-Wave equation Application of staggered leap-frog method Overflow discharge formula for tsunami overflowing by Honma (1940),	
Calculation Grid and Resolution	3240m, 1080m, 360m and 120m without tsunami run-up 40m, 20m and 10m with tsunami run-up Grid nesting calculation for multiple areas	
Roughness Coefficient at the Ground	Reference by Kotani et al. (1998) Sea, River: 0.025, Agricultural field: 0.050, Forest field: 0.030 Residential area: 0.040 (low density), 0.060 (medium density), 0.080 (high density)	
Seismic Slip Model	Fujii and Satake's slip model (ver.4.0) by Fujii et al. (2011)	
Topography	Modified 1994 Iwate Tsunami Prediction Model (Before the earthquake) or Survey data in 2011-2012 (After the earthquake)	
Sea Surface Deformation by the Earthquake	Manshinha & Smylie's Method (1971) Scale factor was calibrated by 1.05-2.90 times from the comparison between estimate value and field survey	
Calculation Period	3 hours from the earthquake outbreak	
Time Resolution	0.1-0.4 sec, dependent on the calculation area	
Coastal Protection Facilities	All of the facilities (Tide wall, River embankment, road embankment) are installed and remaining after the tsunami.	

The accuracy of the model was evaluated by utilizing the values of K and κ in Aida's method (Aida, 1984). The K value indicates consistency between the calculated and observed values, a value of 1.0 reflects identical calculated and observed values, whereas values of 0.8–1.2 reflect highly accurate calculated results. The value of κ indicates the degree of variation; a value

≤1.6 is generally appropriate. In this study, the values of K were in the range 0.97–1.21, and the values of κ were in the range 1.00–1.38. These values suggest that the numerical model provides highly accurate estimates that sufficiently reproduce the observed conditions and that it was possible to proceed with subsequent steps of the study.

The tsunami inundation depth was calculated as the difference between the maximum tsunami height and the elevation for each computational mesh in the GIS. Figure 4 depicts the stepwise process for estimating the tsunami inundation depth. Regional inundation characteristics were subsequently analyzed.

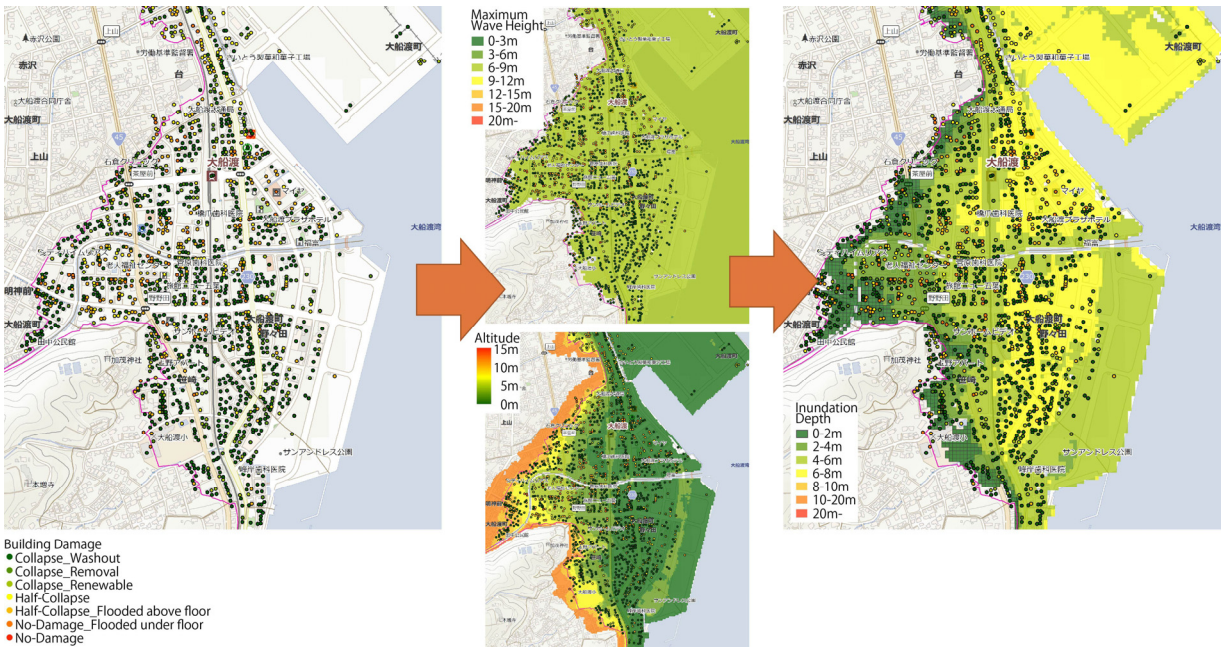

Fig. 4. Tsunami inundation mapping procedure(inundation depth = tsunami height - ground level)

2.4 Building Damage

To support development of the predictive model, building damage characteristics were also obtained from the disaster survey conducted by Japan's MLIT in 2011. In this disaster survey, seven general categories of damage were defined: (1) *collapse_washout*, (2) *collapse_removal*, (3) *collapse_renewable*, (4) *half-collapse_extensive damage*, (5) *half-collapse_flooded above floor*, (6) *no-damage_flood under floor*, and (7) *no-damage_avoid physical damage*. In the current study, three categories of damage we consolidated for the sake of simplicity: (1) *collapse*, (2) *half-collapse*, and (3) *no-damage*. *Collapse* includes washout, removal, and extensive destruction. *Half-collapse* includes flooding above the floor. *No-damage* includes flooding below the floor.

3 Results and Discussion

TABLE 3 summarizes the number of affected buildings, the predominant building structure type, the building density, the tsunami inundation depth, and the predominant building damage characteristics for each of the 27 regional coastal areas considered in this study. Notable regional differences and interdependencies among these factors are discussed below.

TABLE 3. Tsunami inundation and building characteristics in the 27 regional coastal areas
(RC: reinforced concrete; S: steel; W: wood; O/U: others or unknown; Col: collapse; washout/removal/crucial damage; hCol: half-collapse; flooded above floor or extensive damage; and no: no-damage; flooded under floor or less damage)

Area ID	Target area	Major Regional Name	Number of flooded buildings	Building structure [%]				Building density [%]			Extent of damage [%]				Dominant combination of the building structure & damage, and each ratio [%]			Inundation depth [m]
				Reinforced concrete	Steel	Wood	Other/ Unknown	Isolated	Neigh-boring	Surroun-ding	Col	hCol	no	O/U	1	2	3	Most frequent band
1	Hiranai Coast	Taneichi	55	12.7	9.1	69.1	9.1	45.5	43.6	10.9	72.7	27.3	0.0	0.0	W-Col:49.1	W-hCol:20.0	RC-Col:10.9	5-6
2	Yagi Port	Yagi	124	0.0	5.6	90.3	4.0	49.2	43.5	7.3	75.8	22.6	1.6	0.0	W-Col:66.9	W-hCol:21.8	S-Col:5.6	3-4
3	Kuji Bay	Kuji	1,207	3.4	9.1	63.9	23.6	20.1	59.8	20.0	30.9	52.4	16.7	0.0	W-hCol:32.9	W-Col:16.3	W-No:14.7	1-2
4	Noda Coast	Noda	1,055	2.1	0.9	80.9	16.2	14.1	70.3	15.6	64.5	30.0	5.3	0.1	W-Col:50.2	W-hCol:25.6	O/U-Col:12.3	1-2
5	Urube Coast	Otanabe	64	7.8	14.1	67.2	10.9	26.6	71.9	1.6	79.7	20.3	0.0	0.0	W-Col:56.3	W-hCol:10.9	O/U-Col:10.9	7-9
6	Shimanokoshi Coast	Shimanokoshi	230	4.8	1.3	88.3	5.7	10.9	65.7	23.5	97.8	2.2	0.0	0.0	W-Col:86.5	O/U -Col:5.7	RC-Col:4.3	9-10
7	Omoto Coast	Omoto	385	1.8	1.6	52.7	43.9	8.0	41.0	50.9	77.5	21.7	0.8	0.0	O/U -Col:40.0	W-Col:36.4	W-hCol:15.7	3-4
8	Taro Coast	Taro	1,019	2.2	3.0	91.0	3.8	14.5	62.3	23.3	91.6	6.8	1.6	0.0	W-Col:84.4	W-hCol:5.3	O/U-Col:3.7	7-8
9	Osawa Coast	Sakiyama	80	4.1	6.1	79.6	10.2	67.3	32.7	0.0	81.6	13.3	5.1	0.0	W-Col:62.2	W-hCol:12.2	O/U-Col:10.2	4-5
10	Miyako Bay	Miyako	5,252	2.9	7.2	82.3	7.6	10.7	52.0	37.3	53.2	37.3	9.5	0.0	W-Col:46.4	W-hCol:28.3	W-No:7.6	1-2
11	Omoe Coast	Omoe, Otobe	120	0.8	4.2	87.5	7.5	65.8	34.2	0.0	95.8	3.3	0.8	0.0	W-Col:84.2	O/U -Col:7.5	S-Col:3.3	8-9
12	North Yamada Bay	Chikei	50	2.0	0.0	98.0	0.0	80.0	20.0	0.0	98.0	2.0	0.0	0.0	W-Col:96.0	W-hCol:2.0	RC-Col:2.0	9-10
13	Yamada Bay	Yamada	3,736	2.0	5.8	90.6	1.7	8.8	52.8	38.5	87.3	10.7	2.0	0.0	W-Col:78.9	W-hCol:9.8	S-Col:5.3	4-5
14	North Funakoshi Bay	Funakoshi	731	1.9	2.3	90.4	5.3	11.6	57.9	30.5	93.8	5.1	1.1	0.0	W-Col:84.8	O/U -Col:5.1	W-hCol:4.5	11-12
15	South Funakoshi Bay	Kirikiri	703	2.3	1.4	13.5	82.8	17.2	62.2	20.6	93.5	5.3	1.3	0.0	O/U -Col:82.5	W-Col:7.4	W-hCol:5.1	8-9
16	Otsuchi Bay	Otsuchi, Unosumai	6,246	1.7	2.6	17.7	78.1	11.4	53.6	35.0	86.4	13.0	0.6	0.0	O/U -Col:77.5	W-hCol:12.1	W-Col:5.1	7-8
17	Ryoishi Bay	Ryoishi	470	1.7	2.8	5.1	90.4	13.4	37.0	49.6	96.4	3.4	0.2	0.0	O/U -Col:90.4	S-Col:2.8	W-hCol:2.8	17-18
18	Kamaishi Bay	Kamaishi	2,449	12.2	16.0	29.7	42.1	9.8	38.7	51.6	83.7	14.5	1.8	0.0	O/U -Col:41.0	W-Col:21.5	S-Col:12.3	5-6
19	Touni Bay	Kojirahama	634	1.1	3.3	24.0	71.6	25.7	55.8	18.5	89.4	9.3	1.3	0.0	O/U -Col:70.8	W-Col:14.5	W-hCol:8.2	4-5
20	Yoshihama Bay	Yoshihama	36	0.0	2.8	83.3	13.9	58.3	41.7	0.0	94.4	5.6	0.0	0.0	W-Col:80.6	O/U -Col:11.1	S-Col:2.8	10-11
21	Okirai Bay	Okirai	814	1.1	4.7	82.2	12.0	18.1	65.2	16.7	87.2	11.1	1.0	0.7	W-Col:72.9	O/U -Col:10.0	W-hCol:8.1	4-5
22	Ryori Bay	Nonomae	17	0.0	11.8	52.9	35.3	82.4	17.6	0.0	100.0	0.0	0.0	0.0	W-Col:52.9	O/U -Col:35.3	S-Col:11.8	8-9
23	Outer Ofunato Bay	Ryori	461	2.0	4.3	72.7	21.0	16.1	67.7	16.3	77.9	17.8	3.3	1.1	W-Col:55.7	O/U-Col:17.8	W-Col:13.0	2-3
24	Ofunato Bay	Ofunato	5,338	2.9	10.0	71.9	15.2	11.6	58.1	30.3	70.0	25.3	3.7	0.9	W-Col:51.5	W-hCol:16.9	O/U-Col:10.0	4-5
25	Ohno Bay	Massaki	1,400	1.1	3.6	69.6	25.7	11.6	64.0	24.4	87.4	10.3	1.1	1.1	W-Col:58.9	O/U -Col:24.1	W-hCol:9.0	9-10
26	Outer Hirota Bay	Hirota	28	0.0	0.0	21.4	78.6	32.1	67.9	0.0	96.4	3.6	0.0	0.0	O/U -Col:78.6	W-Col:17.9	W-hCol:3.6	6-7
27	Hirota Bay	Rikuzentakata	7,155	1.9	3.1	49.7	45.3	10.4	51.9	37.7	95.2	2.6	0.2	2.0	W-Col:47.0	O/U -Col:43.4	S-Col:3.0	9-10

3.1 Building Structure Type and Damage by Region

Among the 27 coastal areas considered, the percentage of wooden building structures exceeded 80% on Noda Coast, Shimanokoshi Coast, Miyako Bay, Omoe Coast, Yoshihama Bay, and Okirai Bay and 90% in Yagi Port, Taro Coast, North Yamada Bay, Yamada Bay, and North Funakoshi Bay. The percentage of reinforced concrete (RC) and steel building structures exceeded 20% in only three coastal areas—Hiranai Coast, Urube Coast, and Kamaishi Bay. Most of the buildings along the Iwate coast were wooden structures, and most of the wooden buildings or those built with unknown materials were completely destroyed by the tsunami. At South Funakoshi Bay, Otsuchi Bay, Ryoishi Bay, Touni Bay, and Outer Hirota Bay, more than 70% of the building structures were categorized as *other/unknown*. A review of historic aerial photos and satellite images suggests that most of the unknown building structures were in fact wooden structures.

Building damage was minor in only a few regions; in Kuji Bay and Miyako Bay, 16.7% and 9.5% of building structures experienced minor flooding below the floor, respectively. The percentage of building structures avoiding serious damage in the whole of Iwate, including the areas of Kuji Bay and Miyako Bay, was only 2.2%. Thus, most building structures in the study area experienced more than minor damage.

3.2 Building Density by Region

Building density characteristics in the study area were categorized into four types of environments: (1) many isolated buildings (observed on Osawa Coast, Omoe Coast, North Yamada Bay, Yoshihama Bay, and Ryori Bay); (2) combined isolated and neighboring buildings (observed on Hiranai Coast and Yagi Port); (3) combined neighboring and surrounding buildings (observed on Omoto Coast, Miyako Bay, Yamada Bay, North Funakoshi Bay, Otsuchi Bay, Ryoishi Bay, Kamaishi Bay, Ofunato Bay, and Hirota Bay); and (4) many neighboring buildings (observed in Kuji Bay, Noda Coast, Urube Coast, Shimanokoshi Coast, Taro Coast, South Funakoshi Bay, Touni Bay, Okirai Bay, Outer Ofunato Bay, Ohno Bay, and Outer Hirota Bay). Many isolated buildings were located along the narrow, low-lying areas facing the Pacific Ocean. In comparison, higher building densities were observed farther away along the inner part of the enclosed gulf topography.

3.3 Tsunami Inundation and Building Damage by Region

Near the shoreline, most buildings experienced collapse. Farther inland, the percentage of buildings that experienced *half-collapse* or *no-damage* generally increased. Considering the spatial distribution of two coastal areas in detail, many buildings in Kuji Bay were categorized as *half-collapse* and *no-damage* along the flooded seafront as well as in the city center. In comparison, nearly all buildings in Hirota Bay, which is located within 1.5 km of the shoreline, were completely destroyed or carried away by the tsunami outflow. Figure 5 maps the estimated building damage and tsunami inundation depth for these two coastal areas.

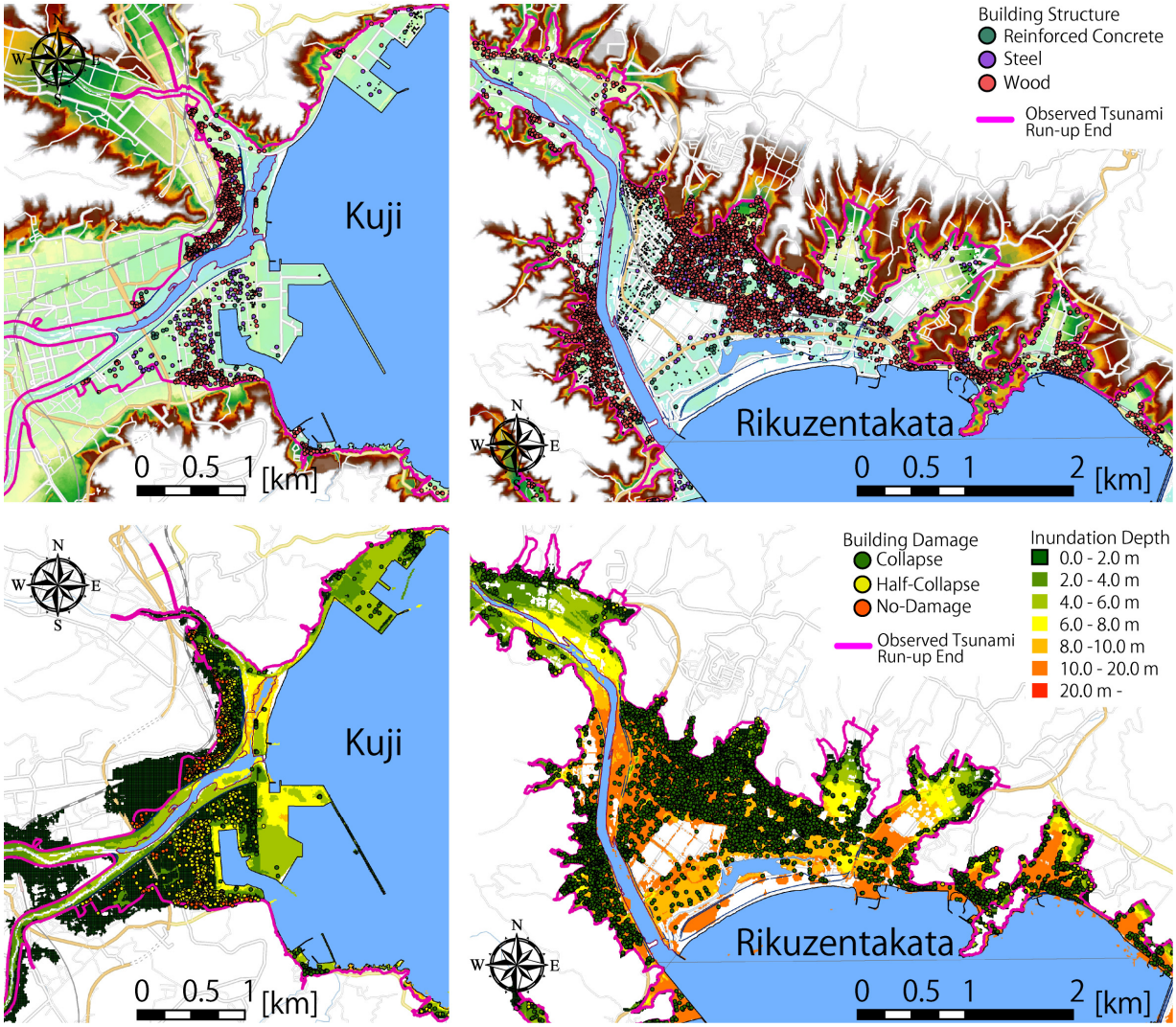

Fig. 5. Building structure type, tsunami inundation depth, and building damage distribution for Kuji Bay (Kuji city) and Hirota Bay (Rikuzentakata city)

In Kuji's city center, 79.5% of the building structures experienced a tsunami inundation depth ≤ 2 m. The tsunami inundation depth was generally higher in Rikuzentakata's city center; 45.8% of the building structures were flooded with 9–11 m of water. Figure 6 shows the relationship between the tsunami inundation depth and building damage. When the tsunami inundation depth exceeded 2 m, the rate of total destruction or *collapse ratio* of wooden building structures in both regions significantly increased and the rate of *no-damage* significantly decreased.

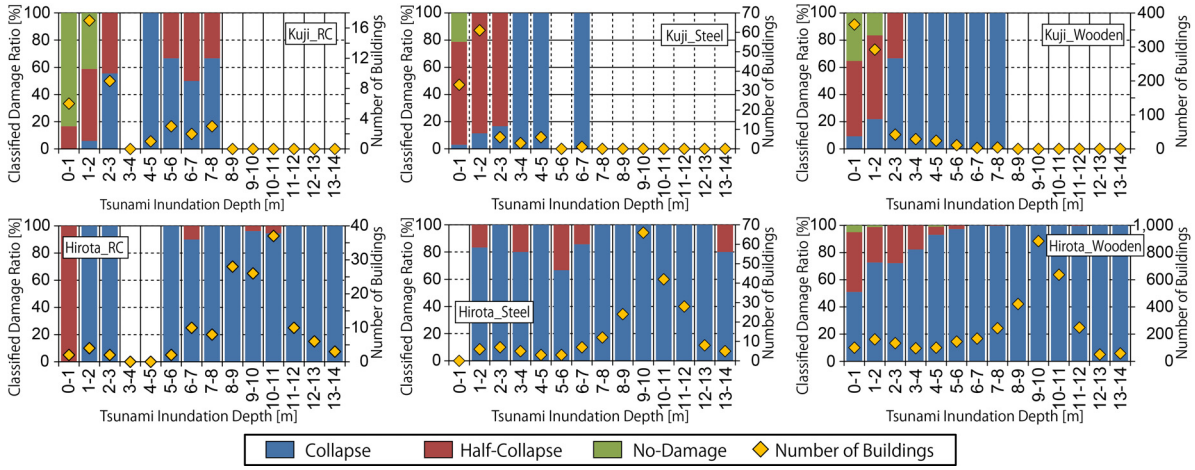

Fig. 6. Comparison of tsunami inundation depth, number of buildings, and their damage for Kuji Bay and Hirota Bay. RC building structure: mainly commercial buildings, schools, city halls, public facilities. Steel building structure: strong high-rise (commercial) and low-rise (housing). Wooden buildings: mainly individual houses and warehouses.

An investigation of tsunami damage by Shuto(1992) found that inundation depths exceeding 1 m and 2 m lead to partial and total destruction, respectively. Koshimura and Gokon (2012a) proposed a tsunami fragility function intended for the buildings affected by the 2011 tsunami in Miyagi Prefecture. They found that the runoff ratio increased rapidly when the inundation depth reached 2 m and approached 80% when the inundation depth reached 6 m. The results from prior tsunami damage investigations are consistent with the results of this study—when the tsunami inundation depth exceeded 2 m, many wooden building structures experienced significant damage—although a direct comparison cannot be made because the affected buildings considered previously differ from those considered in this study with respect to architectural standards.

Regarding RC and steel building structures, the extent of damage to RC buildings was generally lower than the extent of damage to steel buildings for the same tsunami inundation depth.

Despite these noted trends, the determination of a definitive relationship between tsunami inundation depth and building damage was challenged by the limited number of sample cases, the diversity in building designs, the confounding effects of neighboring building structures, and the extent of density conditions.

3.4 Relationship among Inundation Depth and Building Structure Type, Density, and Damage

Based on a damage survey for each building structure within the study area, the collapse ratio at a tsunami inundation depth of 0–1 m was 14.0% for RC structures, 30.1% for steel structures, and 34.2% for wooden structures. The magnitude of the damage differed among these building structure types at the same inundation depths. Many of the affected buildings were damaged beyond repair. Figure 7 shows the collapse ratio as an interaction of the tsunami inundation depth and building density for the three building structure types.

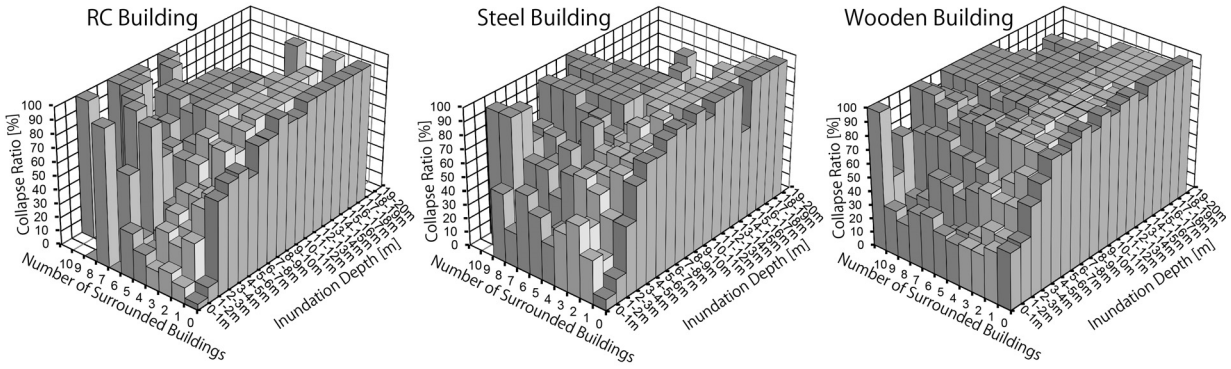

Fig. 7. Relationship among tsunami inundation depth and building structure type, density, and damage at Iwate coast, where "Number of surrounding buildings" signifies the building density, "Inundation depth" is the water height estimated by the tsunami numerical model, and "Collapse ratio" is the proportion of buildings completely destroyed amongthe number of flooded buildings, evaluated according to the three parameters.

For RC building structures and a tsunami inundation depth ≤ 2 m, the collapse ratio in *isolated* (no surrounding buildings) building density environments was 4.3%, whereas the collapse ratios in *neighboring* (1–3 nearby buildings) and *surrounding* (≥ 4 nearby buildings) building density environments were higher. As the tsunami inundation depth increased, the collapse ratios for each building density environment increased until all differences between building density environments were indistinguishable. Isolated RC buildings generally included robust structures used as communal facilities, plants, or high-rise buildings. In comparison, surrounding buildings generally included weaker residential structures with higher associated collapse ratios.

Similar to the RC building structures, the collapse ratio for steel building structures in *isolated* building density environments was lower than the collapse ratios in *neighboring* and *surrounding* building density environments for a tsunami inundation depth ≤ 2 m. When the tsunami inundation depth exceeded 2 m, the collapse ratios again increased sharply. Isolated steel buildings were generally used as commercial, industrial, agricultural, and public facilities. In contrast, surrounding steel buildings were generally intended for residential use.

For wooden building structures and a tsunami inundation depth ≤ 2 m, the collapse ratios were 42.7%, 37.2%, and 30.3% for *isolated*, *neighboring*, and *surrounding* building density environments, respectively. As the building density increased, the collapse ratios decreased. When the tsunami inundation reached 4 m, the collapse ratio for all building density types reached nearly 70%. Wooden building structures were generally used as residences or simple barns for storing fishery equipment. Isolated wooden buildings in coastal areas are directly affected by tsunamis and were severely damaged; however, higher building density areas (e.g., collective housing) were more capable of withstanding the power of the tsunami. Hence, differences in the building structure type, use, and density collectively affect the extent of building damage.

3.5 Building Group Destruction Probability Model Application

In terms of the potential factors related to the geography in TABLE 1, all of the items except for "Coastal Protection Facility" and "Distance to the shoreline" affect the wave height or inundation depth. Because the items "Coastal Protection Facility" and "Distance to the shoreline" did not directly affect buildings, it was thought that they influence the magnitude of building damage as a secondary effect. Regarding potential factors related to the building itself, all of the items directly affected the building resilience to the tsunami. All of the wave parameters expressing the tsunami characteristics were considered to be representable mainly by the depth and range of the inundation. The above items were adopted for the following three reasons: data pertaining to the tsunami simulation results of Iwate Prefecture made it impossible to obtain the velocity and tsunami wave strength in the inundated area; in the process of model development, the goal was to make a reasonable evaluation by combining items that can easily be obtained by ordinary people; items related to the kinetic momentum typified by the tsunami force and flow velocity can be evaluated indirectly to some extent from the inundation depth. However, as pointed out by Park et al., it is necessary to evaluate the kinetic momentum to clarify the influence on a building more strictly (Park et al., 2013). In addition, buildings located in the lower inundation depth zone were greatly influenced in that they experienced damage other than the inundation depth (for example, terrain such as agricultural fields and roads, the presence of walls and trees, and floating cars and houses); thus, evaluation at the lower depth zone has limitations. In order to conduct a more precise evaluation, additional items could be examined and a high-precision numerical model developed. In summarizing these items, the value of "Number of stories" was missing in these areas; hence, its parameters could not be analyzed in this study. In addition, several items focusing on the coastline were excluded from this study. As a result of summarizing the relationship between the building damage characteristics and their factors (selected from the above items), the relationship shown in Fig. 8 was obtained and named the “Building Group Destruction Probability Model.” Fig. 8 is an integration of the empirically obtained on-site data shown in Fig. 7 and it is impossible to improve its functionality because of missing data or unique building characteristics. Therefore, the data were presented as a bar chart estimating the destruction probability with the combination of the following three variables. Explanatory variables included the building structure type (*RC*, *steel*, and *wood*); building density (*isolated*, *neighboring*, and *surrounding*); and the tsunami inundation depth. Fig. 8 depicts the relationship between these explanatory variables and the collapse ratio, which was used to indicate building damage. Because the inundation depth band included missing data above 12 m, the estimated collapse ratio was assumed to be 100% based on proximate data.

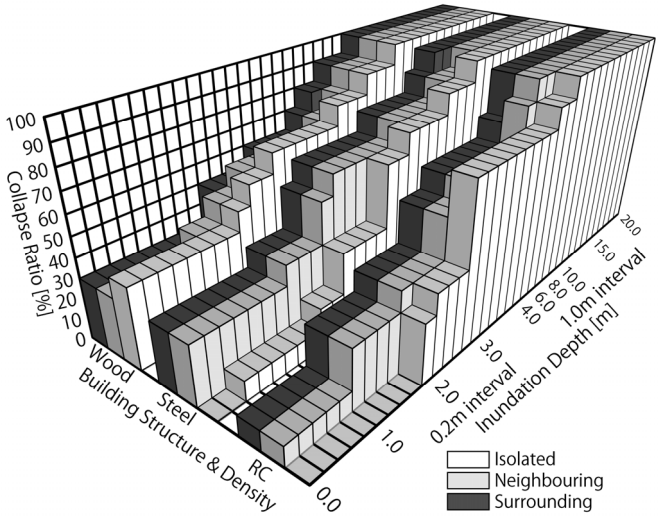

Fig. 8. Proposed building group destruction probability model using building structure type, building density, and tsunami inundation depth as explanatory variables

To test the application of the proposed model, coastal cities in Iwate Prefecture that had > 1,000 tsunami-affected buildings were considered. These cities included Kuji Bay, Noda Coast, Taro Coast, Miyako Bay, Yamada Bay, Otsuchi Bay, Kamaishi Bay, Ofunato Bay, Ohno Bay, and Hirota Bay, shown on the map in Fig. 9. TABLE 4 summarizes the reproducibility of the collapse probability for each area and building structure. In the coastal cities that experienced lower tsunami inundation depths (Kuji Bay, Noda Coast, and Miyako Bay), the collapse probability approaches 100% along the seafront, with the collapse probability declining near the run-up end. Comparing Fig. 9 and Fig. 5 for Kuji Bay, the waterfront area of the tide wall contained a barn and a simple facility for storing fishing equipment. These structures were completely destroyed by the tsunami, and the estimated collapse probability exceeded 90%. The estimated collapse probability in the residential densely populated areas was as low as 30–50% in the Natsui and the Osanai district where houses were densely built around Kuji River. In this area, the actual damage was half-collapse or flooded below the floor, and the estimated value reflected the local situation. In addition, the damaged buildings inundated below the floor that were located on the inland side of the densely populated residential area were approximately 30% or less in this analysis.

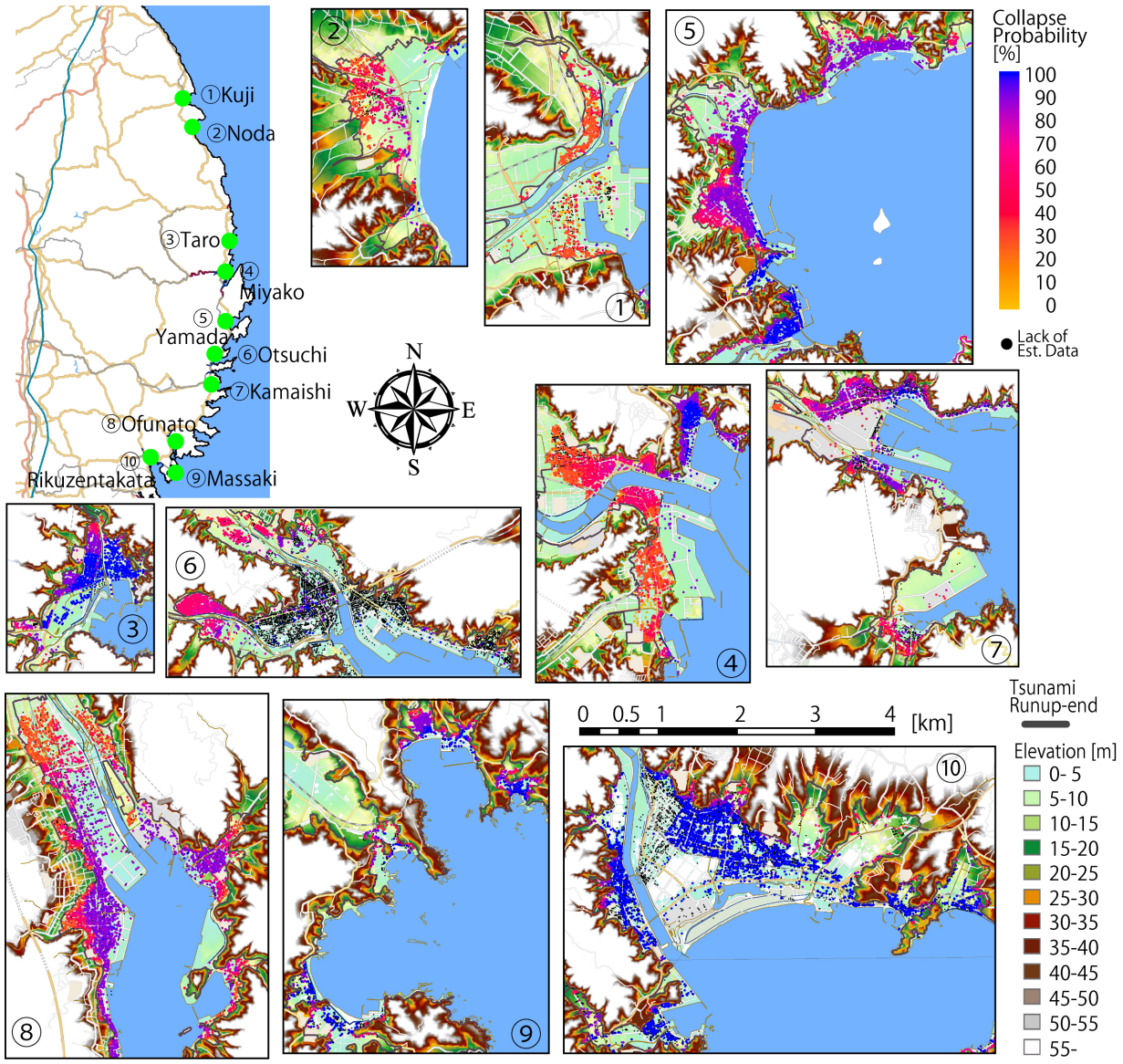

Fig. 9. Spatial distribution of estimated building collapse probability at major coastal cities in Iwate Prefecture

TABLE 4. Mean building collapse ratio reproducibility in the 27 regional coastal areas
(Col = *collapse*, hCol = *half-collapse*, and no = *no-damage*)

Area ID	Reinforced Concrete					Steel					Wood				
	Estimated Mean Collapse Ratio	Actual Mean Collapse Ratio	Number of target buildings with the exception of damage unknown			Estimated Mean Collapse Ratio	Actual Mean Collapse Ratio	Number of target buildings with the exception of damage unknown			Estimated Mean Collapse Ratio	Actual Mean Collapse Ratio	Number of target buildings with the exception of damage unknown		
			Col	hCol	no			Col	hCol	no			Col	hCol	no
1	78.3	85.7	6	1	0	90.0	60.0	3	2	0	81.1	71.1	27	11	0
2	-	-	0	0	0	64.3	100.0	7	0	0	67.8	74.1	83	27	2
3	68.3	29.3	12	17	12	58.4	17.3	19	84	7	57.0	25.6	197	397	177
4	92.9	63.6	14	7	1	91.4	77.8	7	1	1	65.2	62.2	530	270	52
5	100.0	100.0	5	0	0	100.0	33.3	3	6	0	97.5	83.7	36	7	0
6	94.0	90.9	10	1	0	90.0	100.0	3	0	0	91.9	98.0	199	4	0
7	50.0	22.2	2	7	0	76.7	37.5	3	5	0	67.3	69.1	181	78	3
8	96.9	64.0	16	6	3	90.0	69.7	23	10	0	94.4	92.7	939	59	15
9	100.0	100.0	4	0	0	100.0	83.3	5	1	0	88.7	78.2	61	12	5
10	74.3	39.0	60	73	21	76.1	47.3	178	181	17	76.6	56.4	2,437	1,484	401
11	100.0	100.0	1	0	0	85.0	80.0	4	1	0	89.7	96.2	101	3	1
12	40.0	100.0	1	0	0	-	-	0	0	0	86.9	98.0	48	1	0
13	82.2	85.1	63	11	0	84.2	91.7	198	17	1	85.2	87.2	2,949	365	69
14	85.4	92.9	13	1	0	96.3	94.1	16	1	0	87.1	93.8	620	33	8
15	89.3	93.8	15	1	0	89.0	100.0	10	0	0	66.3	54.7	52	36	7
16	92.6	95.2	99	5	0	87.6	87.5	140	19	1	71.8	28.8	318	755	31
17	98.0	62.5	5	3	0	93.1	100.0	13	0	0	82.0	41.7	10	13	1
18	84.6	72.8	217	80	1	81.3	77.0	302	88	2	79.5	72.4	527	168	33
19	86.7	85.7	6	1	0	96.0	95.2	20	1	0	78.8	60.5	92	52	8
20	-	-	0	0	0	90.0	100.0	1	0	0	84.8	96.7	29	1	0
21	85.0	66.7	6	3	0	83.7	78.9	30	8	0	83.1	89.3	593	66	5
22	-	-	0	0	0	70.0	100.0	2	0	0	93.3	100.0	9	0	0
23	77.5	30.8	4	5	4	79.4	80.0	16	4	0	76.7	77.6	257	60	14
24	67.3	70.4	107	38	7	69.5	66.1	351	167	13	70.9	72.2	2,747	902	158
25	82.1	87.5	14	2	0	81.9	96.0	48	1	1	84.4	85.7	825	126	12
26	-	-	0	0	0	-	-	0	0	0	80.0	83.3	5	1	0
27	96.8	95.7	132	6	0	94.8	97.7	213	5	0	93.9	95.5	3,362	152	8

On the other hand, in the areas where the depth of flooding closely behind the tide wall was less than 2 m, the building damage was assumed to be low; but in reality, many wooden buildings collapsed. There were few such cases compared to the total number of buildings included in the sample, but they were underestimated compared to building damage with the same tsunami inundation depth, building density, and building structure. Furthermore, items other than the parameters presented in this paper may have a great influence. These results were qualitatively consistent with the observation. In low-lying areas between the shoreline and the mountain foothills that experience higher tsunami inundation depths (Taro Coast, Ohno Bay, and Hirota Bay), the collapse probability was estimated to be higher, consistent with observation. When the reproducibility in Hirota Bay (Fig. 5 and Fig. 9) was examined in detail, the proportion of total destroyed buildings against the total number of buildings by structure was 95.7%, 97.7%, and 95.5% in RC, Steel, and Wood, respectively. The mean collapse probability was 96.8%, 94.8%, and 93.9%, respectively, which is similar (TABLE 4). In particular, the estimated collapse probability for buildings that actually collapsed on ground ranging from flat to loose slopes was more than 90%, thus reproducing the actual situation. In sloped areas, the extent of damage decreased with an increase in altitude, and the estimated collapse probability decreased from 80% to 30%. In the vicinity of the tsunami run-up end, where the altitude was higher, although buildings with low reproducibility of the estimated damage ratio could be confirmed, it is suspected that the accuracy of the tsunami numerical simulation was attributed to it. Urube Coast, Shimanokoshi Coast, Taro Coast, Omoe Coast, North Yamada Bay, North Funakoshi Bay, Ryoishi Bay, Yoshihama Bay, and Ohno Bay have terrain similar to that of Hirota Bay and higher tsunami inundation depths. The collapse probabilities in these regions were also estimated to be high. The estimated collapse probabilities for Otsuchi Bay and Yamada Bay were more moderate. Beyond the tsunami run-up end, building damage dramatically declined with an estimated collapse probability 40–80%. A higher proportion of RC and steel building structures existed within the Kamaishi Bay and Ofunato Bay tsunami inundation areas. Estimated collapse probabilities differed for RC and steel building structures compared with wooden building structures. The proposed model estimated low collapse probabilities for isolated RC buildings in relatively high tsunami inundation depth zones. Moreover, the proposed model estimated high collapse probabilities for densely arranged steel buildings in lower inundation depth zones. Both results are consistent with observations based on building structure type, use, and density. Hence, the proposed empirical model can be qualitatively confirmed to predict tsunami damage risk; building damage estimation can be further enhanced by considering the building arrangement and building group aspects.

To quantitatively assess the proposed model, areas with a higher proportion of wooden building structures and higher associated collapse ratios offer greater reproducibility. Candidate areas included Shimanokoshi Coast, Taro Coast, Omoe Coast, North Yamada Bay, North Funakoshi Bay, Yoshihama Bay, Okirai Bay, Ryori Bay, and Rikuzentakata (Kuji Bay, Miyako Bay, Otsuchi Bay, and Ryoishi Bay have lower wooden building proportions). The mean differences between the observed and estimated collapse ratios for all target buildings were 8.2%, 5.9%, and 5.1% for RC, steel, and wooden building structures, respectively.

Some geographical features challenged the performance of the model. The reproducibility of building damage was relatively low for the affected buildings behind the seawall in Kuji Bay, Miyako Bay, in the vicinity of the tsunami run-up border in Ofunato Bay, Otsuchi Bay, and other areas. Both the buoyancy generated by the increased tsunami inundation depth and the wave energy applied to the seawall (proportional to the inundation depth magnitude) are considered to affect the estimation results. Behind the seawalls, wave energy proportional to the inundation depth magnitude and kinetic energy induced by potential energy during tsunami overflow are assumed to

act on the buildings. Thus, consideration of the maximum inundation depth alone may not adequately determine the energy applied to a building immediately behind the seawall. In areas near the tsunami run-up border where inundation depths are shallow, the extent of flooding is affected by the microtopography and the presence or absence of buildings. Referenced tsunami calculation models were modified to account for the influence of buildings. These improvements to the tsunami run-up model were expected to enhance the reproducibility near the tsunami run-up border and in shallow flooding regions.

The tsunami inundation depth can be estimated under a variety of scenarios using a numerical model to obtain the building density. Therefore, these damage estimation methods and parameters can be used to assess disaster risk in other regions. Because this study focused on conditions in the coastal areas of Iwate Prefecture with a high proportion of low-rise, wooden building structures, application to urban areas comprising more high-rise buildings may require additional research and review.

5 Conclusion

This study examined the regional spatial characteristics of flooding and building damage incurred during the tsunami following the GEJE of 2011 using GIS and an analytical model. The model, which evaluates total building destruction risk, was developed using building damage data from the coastal areas of Iwate Prefecture. The following results were obtained:

(1) As an overall trend, a higher proportion of collapsed buildings was observed near the shoreline; in contrast, higher proportions of buildings that were partially collapsed or had no damage were observed inland. A spatial survey of the difference between the building damage in two coastal areas revealed that a tsunami inundation depth of 9–11 m affected 45.8% of the buildings in Hirota Bay, whereas a tsunami inundation depth of ≤ 2 m was found to affect 79.5% of the buildings in Kuji Bay. Their unique topographical features were thought to account for the difference in damage.

(2) Collapse ratios differed based on the building structure type, use, density, and tsunami inundation depth. Isolated RC and steel buildings experienced less damage than those in higher density environments for tsunami inundation depths ≤ 2 m. In comparison, under the same tsunami inundation depth conditions, isolated wooden buildings had a higher collapse ratio than higher density environments.

(3) Based on the building characteristics in the coastal areas of Iwate Prefecture, the total building destruction risk was examined and a predictive model was developed. This model was proven capable of estimating the building collapse ratio using the building structure type, building density, and extent of tsunami inundation as explanatory variables.

This study represents an initial step in correlating tsunami and building damage characteristics. To enhance these results, additional small-scale investigations considering the tsunami inundation depth, tsunami speed, detailed coastal geography, building distribution, among other factors, should be conducted. New findings are expected to enable the development of a more sophisticated numerical model.

Acknowledgements

Field survey data were provided by Japan's Ministry of Land, Infrastructure, Transport, and Tourism and the Geospatial Information Authority. The output of the numerical simulation model for the tsunami was provided by Iwate Prefecture. This work was supported by the Japan Society for the Promotion of Science (JSPS) Grants-in-Aid for Scientific Research (KAKENHI) Program (Grant Number 15K20849) and the Takahashi Industrial and Economic Research Foundation.

References

Aida, I., 1984. A source model of the tsunami accompanying the 1983 Nihonkai-Chubu earthquake, *Bulletin of the Earthquake Research Institute—University of Tokyo,* 59, 93–104.

Arikawa, T., 2012. Tsunami disaster due to the Great Eastern Japan Earthquake, Concr. J., 50(1), 23–29.

Charvet, I., I. Ioannou, T. Rossetto, A. Suppasri, and F. Imamura, 2014. Empirical fragility assessment of buildings affected by the 2011 Great East Japan tsunami using improved statistical models, Nat. Hazards, 73(2), 951–973.

Fujii, Y., K. Satake, S. Sakai, M. Shinohara, and T. Kanazawa, 2011. Tsunami source of the 2011 off the Pacific coast of Tohoku Earthquake, Earth Planets Space, 63, 815–820.

Geospatial Information Authority of Japan—Ministry of Land, Infrastructure, Transport, and Tourism. 2012. Maps and geospatial information. http://www.gsi.go.jp/kiban (accessed October 26, 2015).

Gokon, H., S. Koshimura, and M. Matsuoka, 2016. Integration of building unit based andzonal based approaches to detect washed-away buildings in a tsunami affected area using TerraSAR-X data, J. Japan Assoc. Earthq. Eng., 16(3), 147–156.

Hatori, T., 1964. A study of the damage to houses due to a tsunami, Bull. Earthq. Res. Inst., 42, 181–191.

Hiraishi, H., 2012. Outline of damage by Tohoku-Chiho Taiheiyo-Oki earthquake (buildings), Concr. J., 50(1), 4–12.

Honma, H., 1940. Coefficient of flow volume on low overflow weir, Civil Eng., 26(6), 635 645 (in Japanese).

Inukai, N., T. Hosoyamada, M. Lu, T. Kumakura, M. Minami, and H. Irie., 2012. The survey of the north Iwate area due to the 2011 off the Pacific coast of Tohoku earthquake, J. Japan Soc. Civil Eng. B3, 68(2), 19–24.

Iwate Prefecture. 2011–2012. Tech. Commit. Tsunami Disaster Prevent. Technol. Proc., 1–8.

Japan Meteorological Agency. 2012. Report on the 2011 Off the Pacific Coast of Tohoku Earthquake, Tech. Rep. Japan Meteorol. Agency, No.133, pp. 354.

Kawasaki, K., 2012. Fundamental characteristics of tsunami and tsunami disaster due to the 2011 off the Pacific Coast of Tohoku Earthquake, Japanese J. Multiphase Flow, 26(1), 11 18.

Koshimura, S., and H. Gokon, 2012a. Structural vulnerability and tsunami fragility curves from the 2011 Tohoku Earthquake tsunami disaster, J. Japan Soc. Civil Eng. B2, 68(2), I_336–I_340.

Koshimura, S., H. Gokon, T. Fukuoka, and S. Hayashi, 2012b. Remote sensing and GIS-based approach to identify the impact of the 2011 Tohoku Earthquake tsunami disaster, J. JapanAssoc. Earthq. Eng., 12(6), 50–62.

Kotani, M., F. Imamura, and N. Shuto, 1998. Tsunami run-up simulation and damage estimation by using GIS. Proc. Coastal Eng., Japan Soc. Civil Eng., 45, 356–360 (in Japanese).

Macabuag, J., T. Rossetto, I. Ioannou, A. Suppasri, D. Sugawara, B. Adriano, F. Imamura, and S. Koshimura, 2016. A proposed methodology for deriving tsunami fragility functions for buildings using optimum intensity measures, Nat. Hazards, 84 (2), 1257–1285.

Mansinha, L., and D. E. Smylie, 1971. The displacement fields of inclined faults, Bull. Seismol. Soc. America, 61(5), 1433–1440.

Mori, N., and T. Takahashi, 2012. The 2011 Tohoku Earthquake Tsunami Joint Survey Group nationwide post event survey and analysis of the 2011 Tohoku earthquake tsunami, Coast. Eng. J., 54(1), 1–27. doi:10.1142/S0578563412500015.

Narita, Y., and S. Koshimura, 2015. Classification of tsunami fragility curves based on regional characteristics of tsunami damage, J. Japan Soc. Civil Eng. B2, 71(2), 331–336.

Park, H., D. T. Cox, P. J. Lynett, D. M. Wiebe, and S. Shin, 2013. Tsunami inundation modeling in constructed environments: A physical and numerical comparison of free-surface elevation, velocity, and momentum flux, Coast. Eng., 79, 9–21.

Suppasri A., E. Mas, S. Koshimura, K. Imai, K. Harada, and F. Imamura, 2012. Developing tsunami fragility curves from the surveyed data of the 2011 Great East Japan Tsunami in Sendai and Ishinomaki plains, Coastal Eng. J., 54(1), 1250008. doi: 10.1142/S0578563412500088

Shuto, N., 1993. Tsunami intensity and disasters, tsunamis in the world, Adv. Nat. Technol. Hazards Res., 197–216.

Suzuki, T., J. Sasaki, Y. Tajima, and K. Hayano, 2012. Field survey of the 2011 off the Pacific coast of Tohoku earthquake tsunami disaster to the south of Iwate prefecture, J. Japan Soc. Civil Eng. B3, 68(2), 25–30.

Yanagawa, R., and S. Sakai, 2014a. Topographical, propagating tsunami and affected building features by the Great East Japan Earthquake tsunami in the Iwate coastal region, J. Japan Soc. Nat. Disaster Sci., 33(2), 145–159.

Yanagawa, R., and S. Sakai, 2014b. Relational analysis between tsunami and house damage at the inundation area in Iwate, Japan. Proc. 34th Int. Conf. Coast. Eng., Seoul, Korea.

Yanagawa, R., and S. Koshino, 2016. Tsunami inundation area and run-up height in the Iwate coastal region following the Great East Japan Earthquake as estimated from aerial photographs and digital elevation data, Nat. Hazards, 82(3), 2051–2073. DOI:10.1007/s11069-016-2285-1.